2009 fall

# Phase Transformation of Materials

10.27.2009

Eun Soo Park

Office: 33-316
Telephone: 880-7221
Email: espark@snu.ac.kr
Office hours: by an appointment

# Contents for previous class

## 3.4 Interphase Interfaces in Solids

**Interphase boundary - different two phases : different crystal structure**
**different composition**

coherent, **Perfect atomic matching at interface**

$\gamma$ **(coherent) =** $\gamma_{ch}$   $\gamma$ **(coherent) ~ 200 mJM$^{-2}$**

semicoherent $\gamma(semicoherent) = \gamma_{ch} + \gamma_{st}$

$\gamma_{st}$ **→ due to structural distortions caused by the misfit dislocations**

$\gamma$**(semicoherent) ~ 200~500 mJM$^{-2}$**

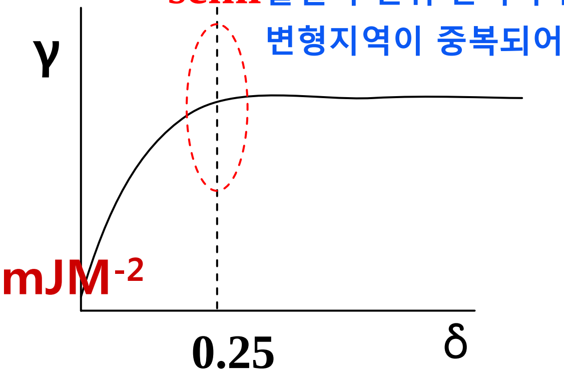


**δ=4: 1 dislocation per 4 lattices**

incoherent

**1) δ > 0.25** 격자가 잘 일치하는 것이 불가능해짐

**2) different crystal structure (in general)**

$\gamma$ **(incoherent) ~ 500~1000 mJM$^{-2}$**

Complex Semicoherent Interfaces

**Nishiyama-Wasserman (N-W) Relationship**

**Kurdjumov-Sachs (K-S) Relationships**



(두 방위관계의 유일한 차이점은 조밀면에서 5.26°만큼 회전시킨 것임)

# Contents for today's class

- **Interphase Interfaces in Solid (α/β)**

  - **Second-Phase Shape** { **Interface Energy Effects** / **Misfit Strain Effects** }

  - **Coherency Loss**

  - **Glissil Interfaces**

  - **Solid/Liquid Interfaces**

- **Interphase migration**

  - **Diffusion controlled and Interface controlled growth**

# 3.4.2 Second-Phase Shape: Interfacial Energy Effects

**How is the second-phase shape determined?** $\sum A_i \gamma_i = minimum$

여러가지 다른 종류의 석출물에 대해 어떻게 자유에너지 최소화 시킬 수 있는지...

## A. Fully Coherent Precipitates

(G.P. Zone)

- If α, β have the same structure & a similar lattice parameter
- Happens during early stage of many precipitation hardening
- Good match ⇨ can have any shape ⇨ spherical

(a)

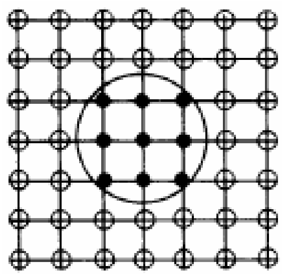

(b)

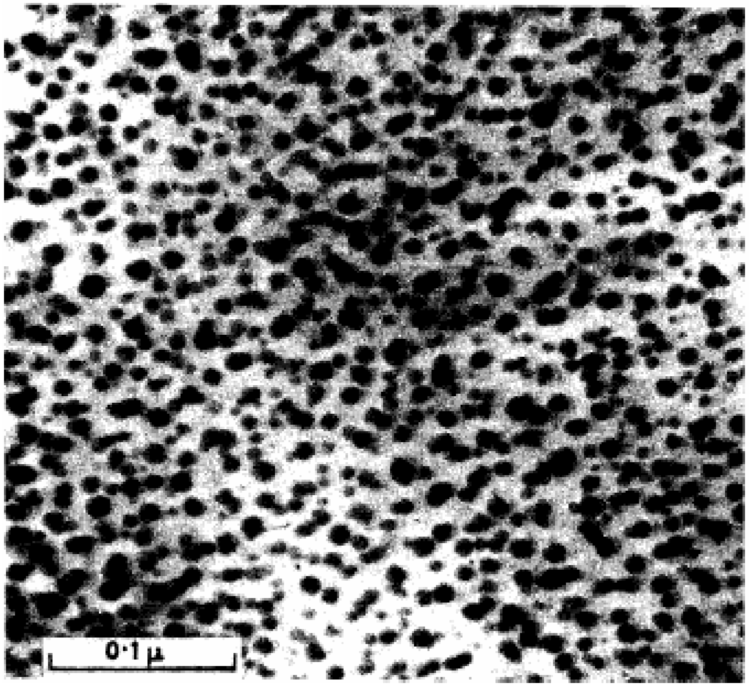


GP(Guinier- Preston) Zone
in Al – Ag Alloys

$$\varepsilon_a = \frac{r_A - r_B}{r_A} = 0.7\%$$

→ negligible contribution
to the total free energy

지름 약 10 nm인 GP 대: Al-rich FCC 기지내
Ag-rich FCC 석출물 형성

## B. Partially Coherent Precipitates

- α, β have different structure and one plane which provide close match

- <u>Coherent or Semi-coherent in one Plane</u>;
  Disc Shape (also plate, lath, needle-like shapes are possible)

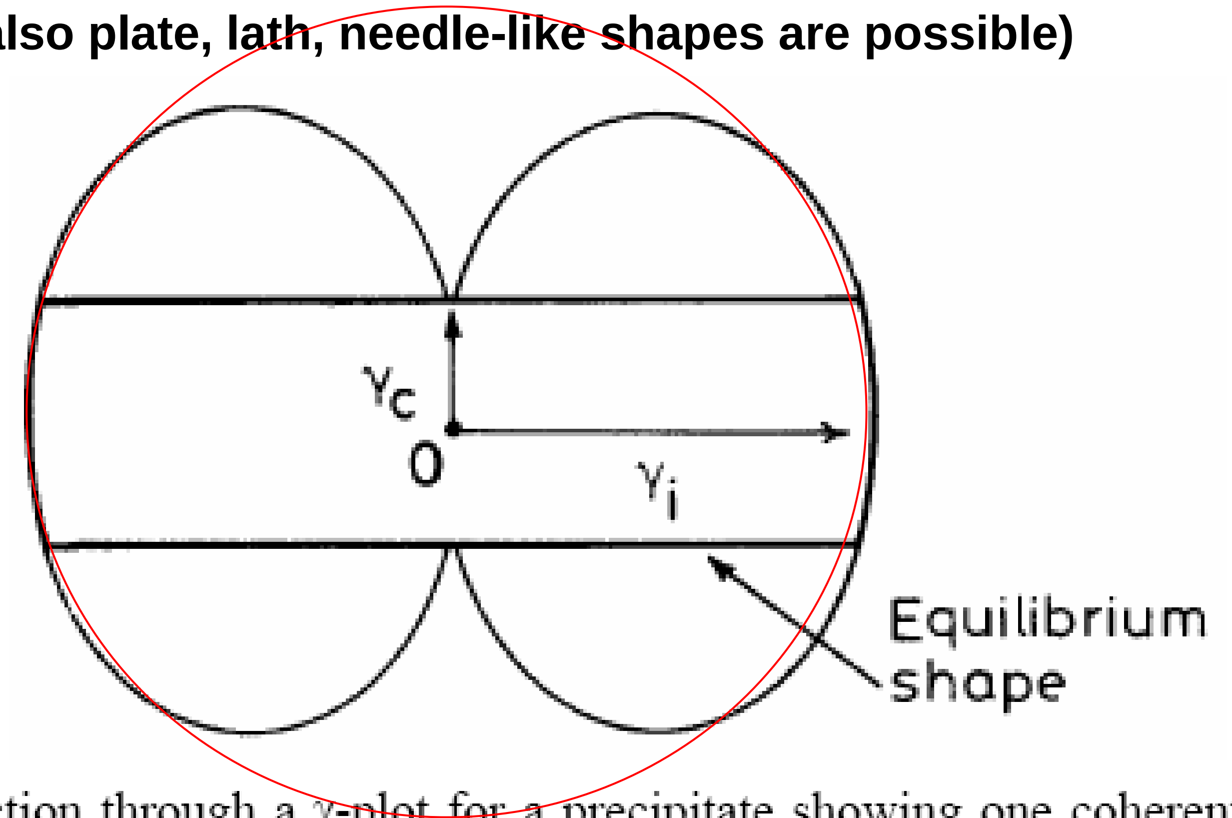


Fig. 3.40 A section through a γ-plot for a precipitate showing one coherent or semicoherent interface, together with the equilibrium shape (a disc).

실제 석출물의 모양 disc 모양 아님. 그 이유는 1) 불일치의 변형 에너지가 무시됨
2) 석출물의 방향에 따라 성장속도 다름

# hcp $\gamma'$ Precipitates in $Al - 4\% Ag$ Alloys $\rightarrow$ plate

**broad face parallel to the $\{111\}_\alpha$ matrix planes** Hcp/Fcc의 방위관계 가지는 판상

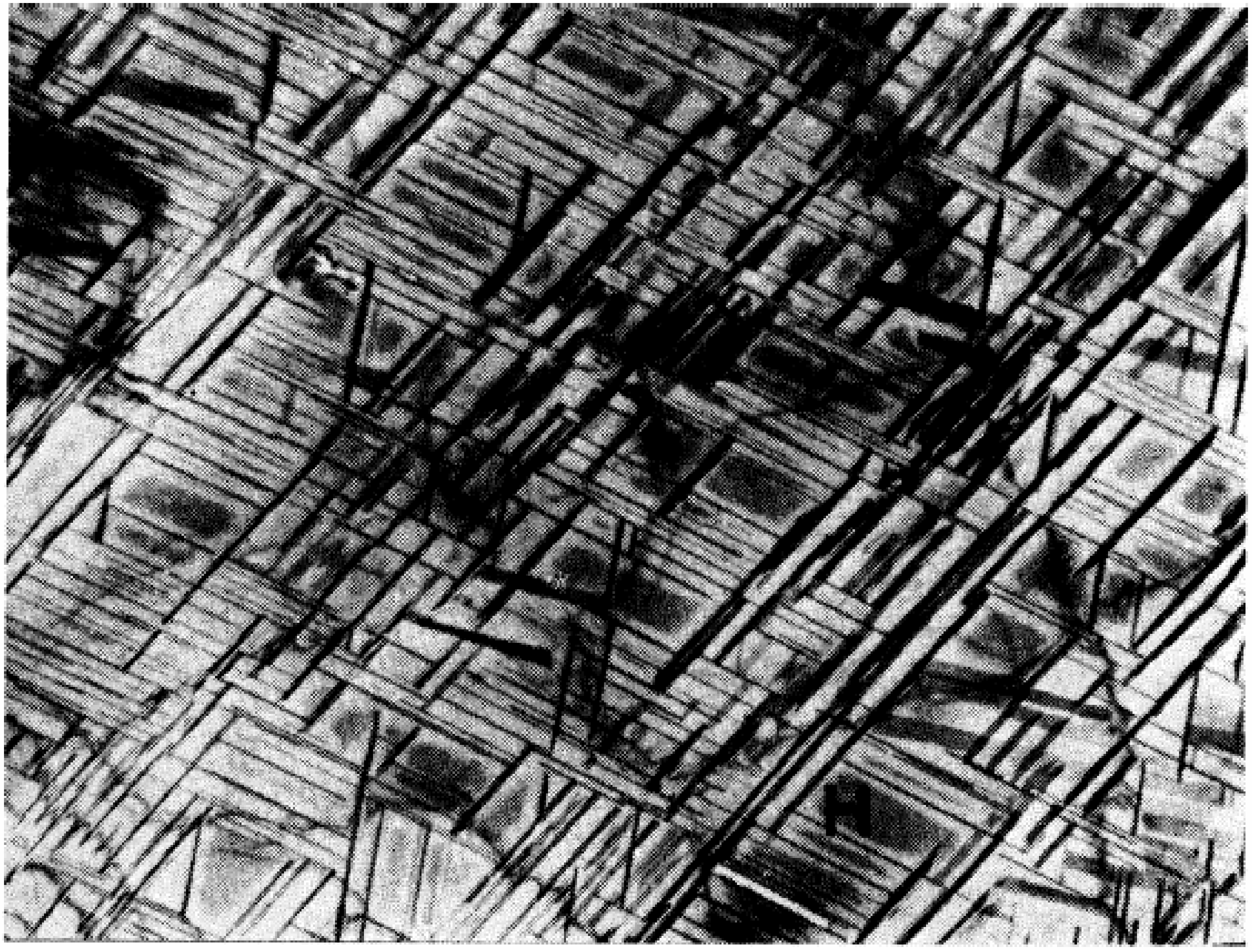

Fig. 3.42 Electron micrograph showing the Widmanstätten morphology of $\gamma'$ precipitates in an Al-4 atomic % Ag alloy. GP zones can be seen between the $\gamma'$, e.g. at H (× 7000). (R.B. Nicholson and J. Nutting, Acta Metallurgica, 9 (1961) 332.)

# $\theta'$ Phase Al–Cu Alloys

**broad face parallel to the $\{100\}_\alpha$ matrix planes** (habit plane)

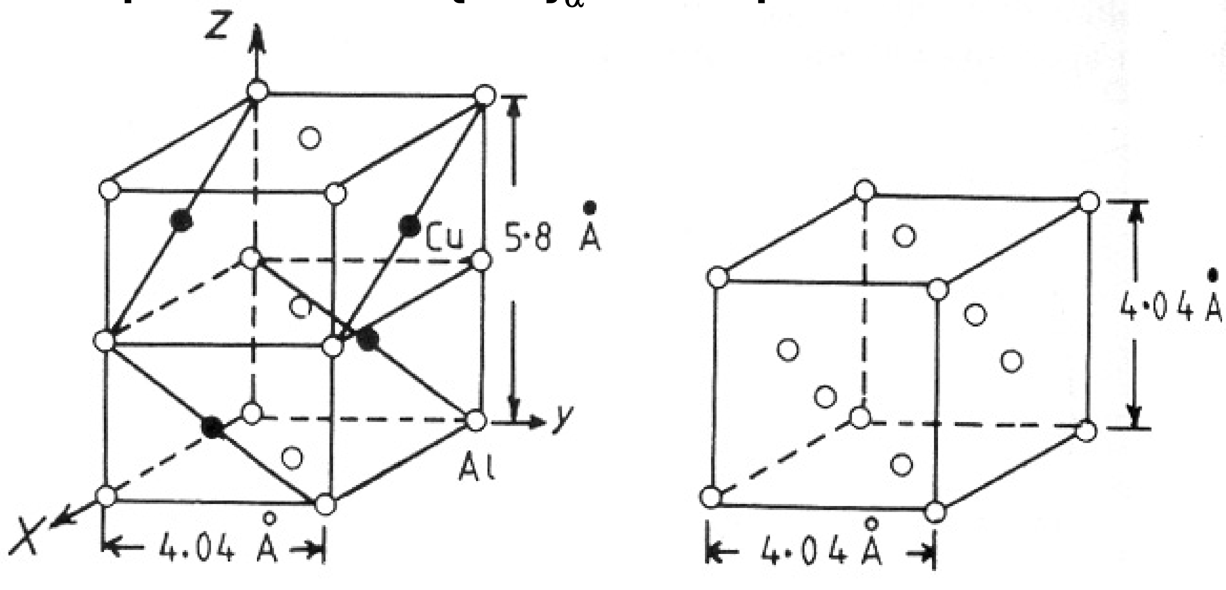


(a) Θ' 석출물 단위격자 (b) Matrix의 단위격자

$$(001)_{\theta'} \; // \; (001)_\alpha \qquad [100]_{\theta'} \; // \; [100]_\alpha$$

→ Al 많이 포함한 기지 (α) 입방대칭이어서
주어진 결정립 내 여러 방향에서 방위를 만족하는 판상 석출물 존재

S phase in Al-Cu-Mg alloys ; Lath shape

$\beta'$ phase in Al-Mg-Si alloys ; Needle shape

} **Widmanstätten morphology**

## C. Incoherent precipitates

- when α, β have completely different structure ⇨ Incoherent interfaces

  or When the two lattices are in a random orientation

- Interface energy is high for all plane ⇨ spherical shape

- Polyhedral shapes : 석출물의 어떤 결정면이 γ-plot의 변곡점 위에 놓이는 경우

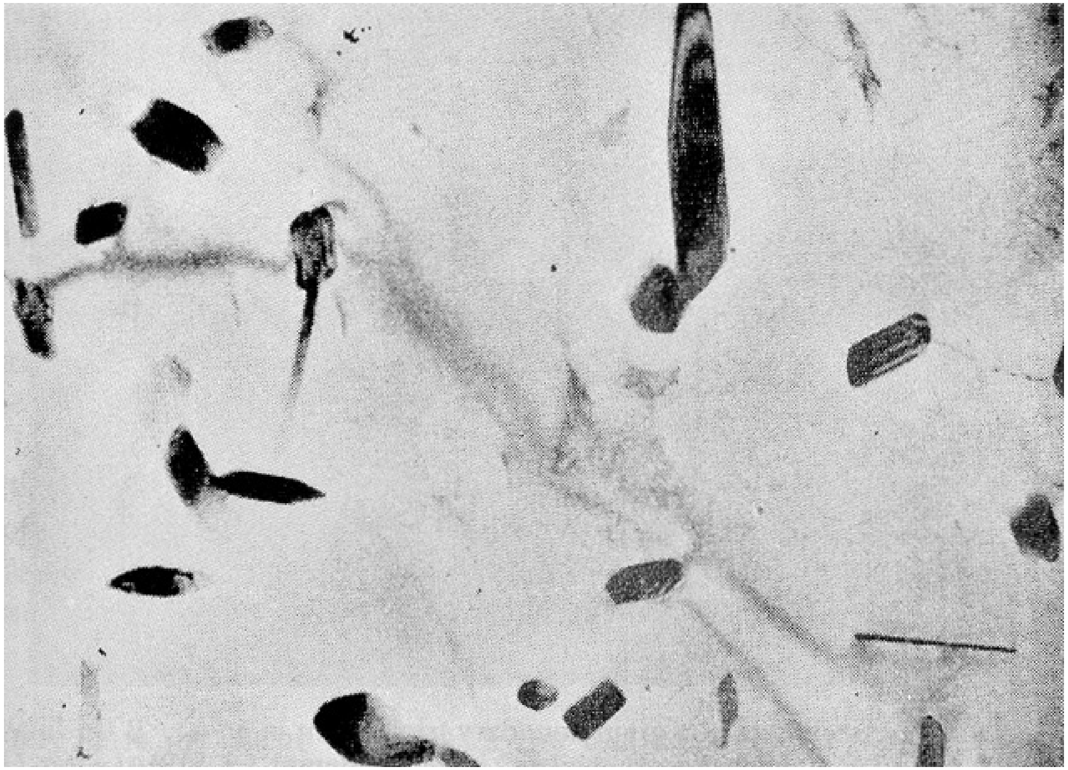

$\theta$ phase in $Al-Cu$ alloys (Al2Cu)

# Precipitation Hardening

- Ex: Al-Cu system
- Procedure:

- *Pt A*: *solution heat treat (get a solid solution)*

- *Pt B*: *quench to room temp.*

- *Pt C*: *reheat to nucleate small θ crystals within α crystals.*

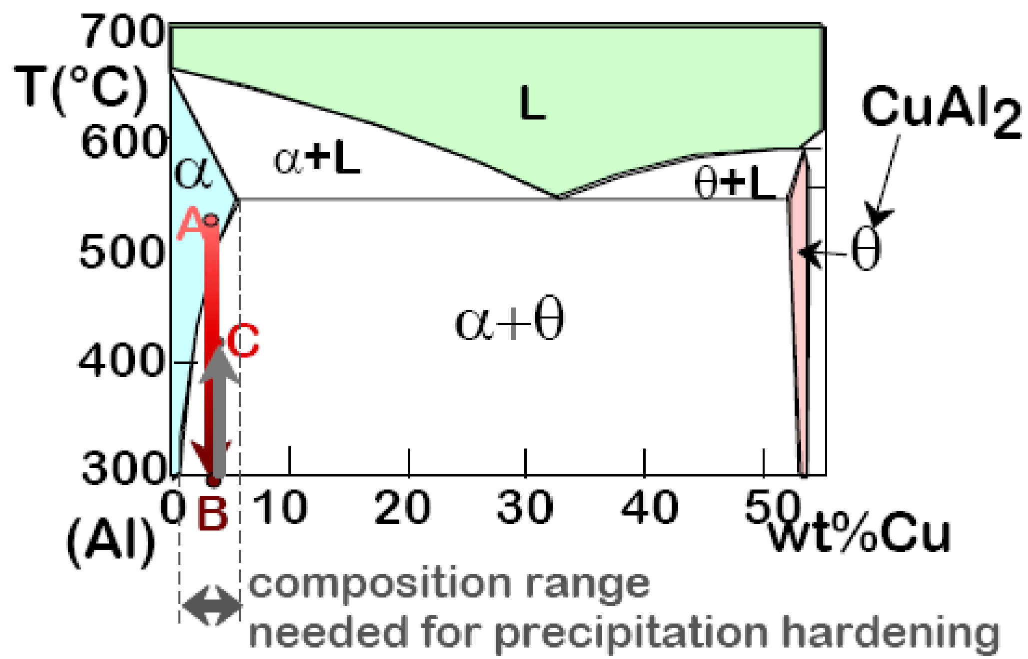


$\alpha + \theta \rightarrow$ Heat (~550°C) $\rightarrow$ Quench (0°C) $\rightarrow \alpha$ (ssss) $\rightarrow$ Heat/age (~150°C) $\alpha + \theta_{ppt}$

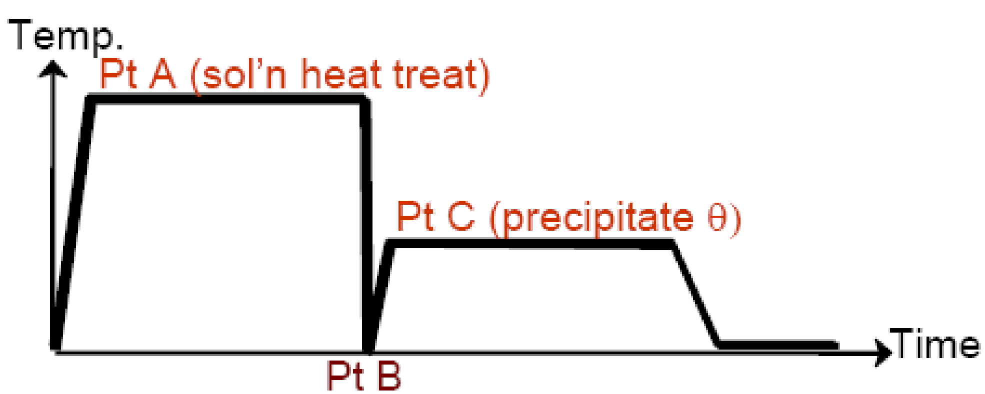

# Al-Cu ppt structures

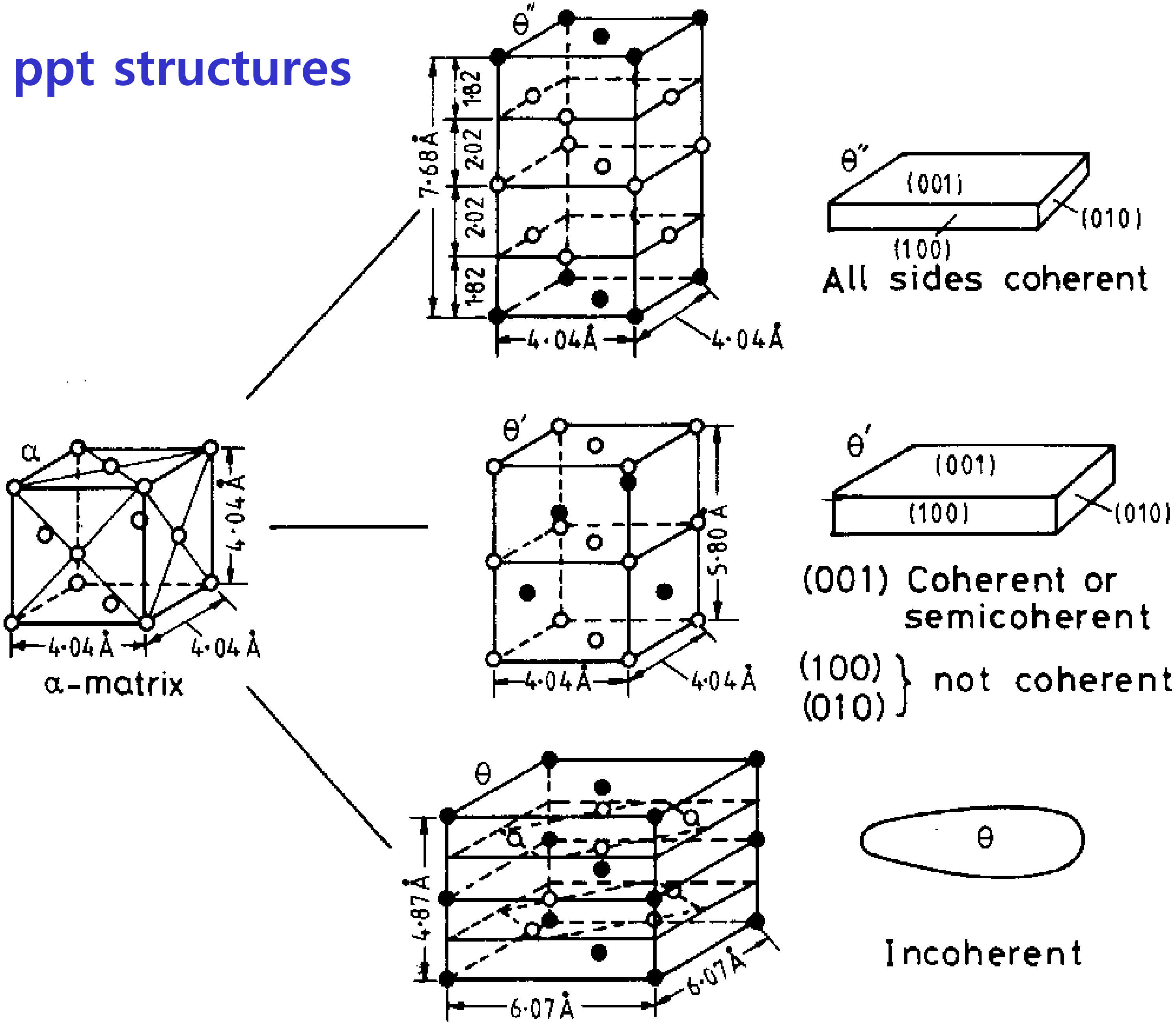


Fig. 5.29 Structure and morphology of θ″, θ′ and θ in Al–Cu (○ Al, ● Cu).

# Al-Cu ppt structures

GP zone structure

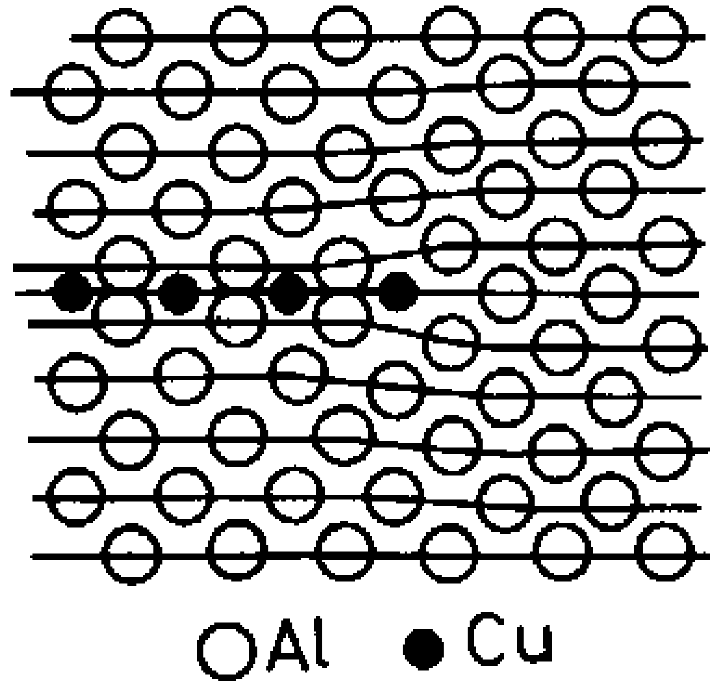


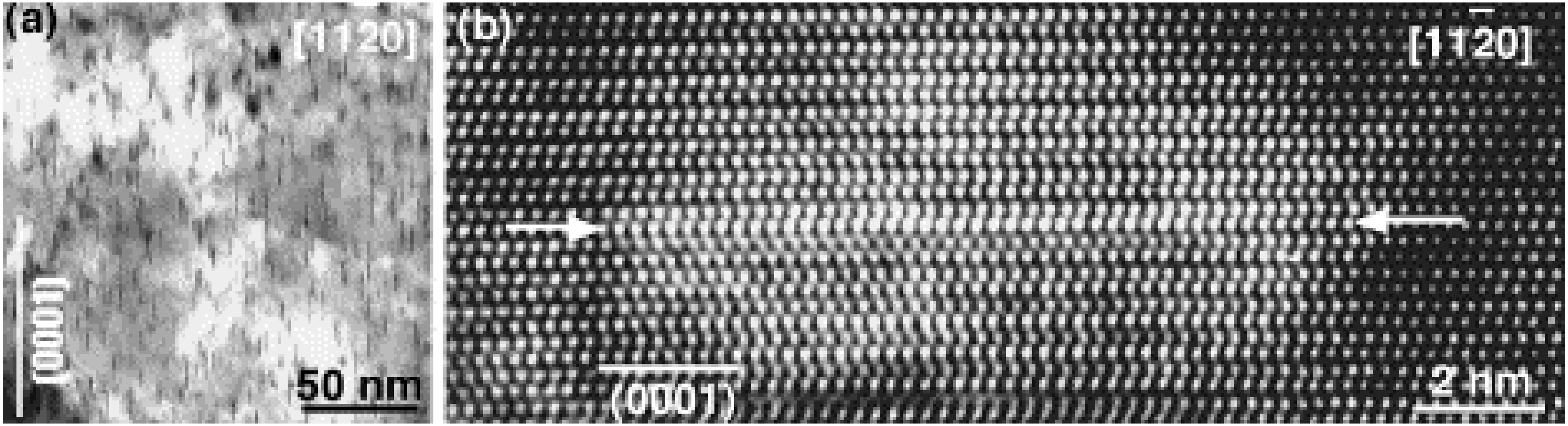


**(a) Bright-field TEM image showing G.P. zones, and (b) HRTEM image of a G.P. zone formed on a single (0 0 0 1)$_\alpha$ plane. Electron beam is parallel to in both (a) and (b).**

# $\theta$ phase in $Al-Cu$ alloys ($Al_2Cu$)

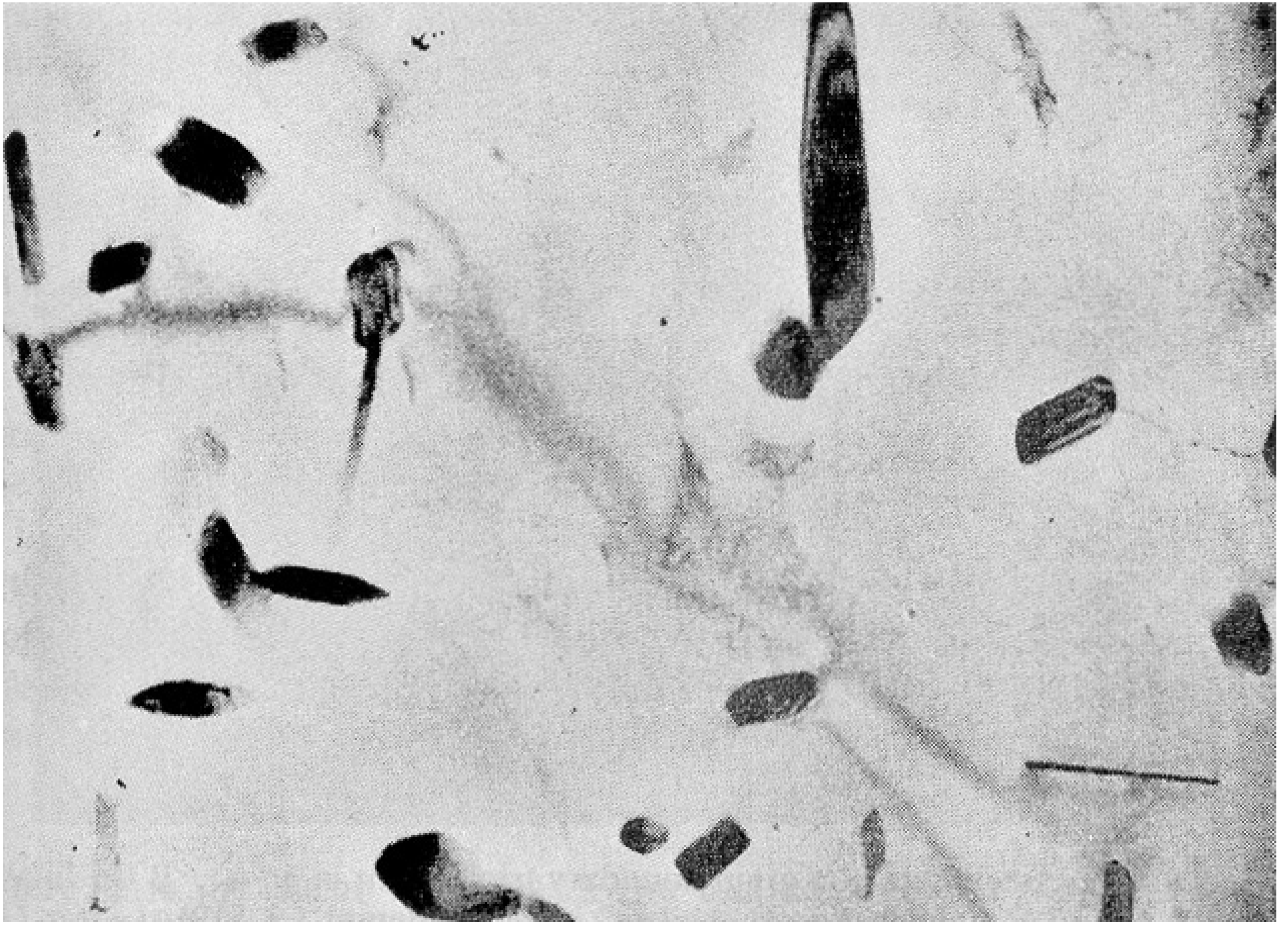

- **Polyhedral shapes : 석출물의 어떤 결정면이 γ-plot의 변곡점 위에 놓이는 경우**

# Precipitates on Grain Boundaries

다른 방위를 갖는 2 개의 결정립 사이의 입계에서 제 2 상의 형성

1) incoherent interfaces with both grains

2) a coherent or semi-coherent interface with one grain and an incoherent interface with the other,

3) coherent or semi-coherent interface with both grains

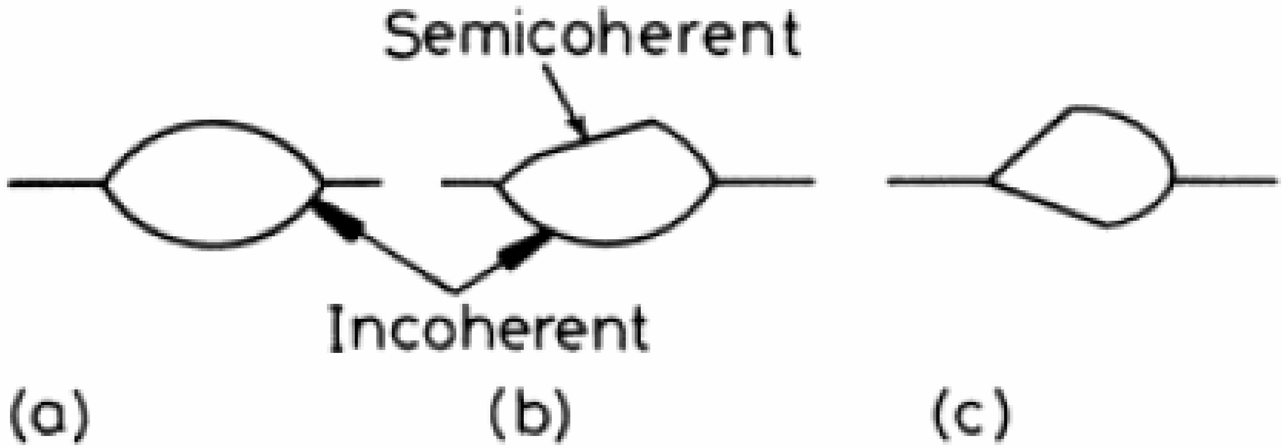


Fig. 3.45 Possible morphologies for grain boundary precipitates. Incoherent interfaces smoothly curved. Coherent or semicoherent interfaces planar.

## Precipitates on Grain Boundaries

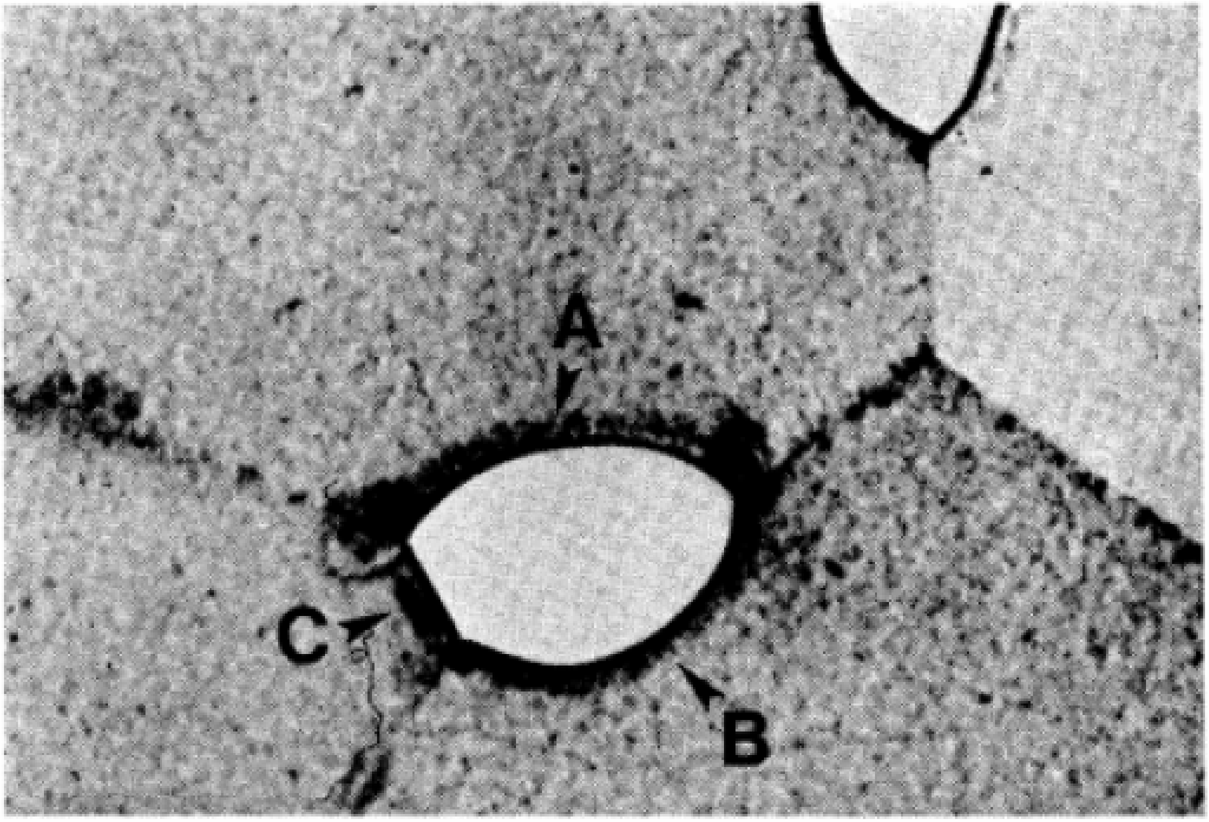


Fig. 3.46 An α precipitate at a grain boundary triple point in an α − β Cu-In alloy. Interfaces A and B are incoherent while C is semicoherent (× 310). (After G.A. Chadwick, *Metallography of Phase Transformations*, Butterworths, London, 1972.)

A, B; Incoherent, C; Semi-coherent

# 3.4.3. Second-Phase Shape: Misfit Strain Effects

$$\sum A_i \gamma_i + \Delta G_S = minimum$$

Elastic strain energy

## A. Fully Coherent Precipitates

석출물 격자상수 다름

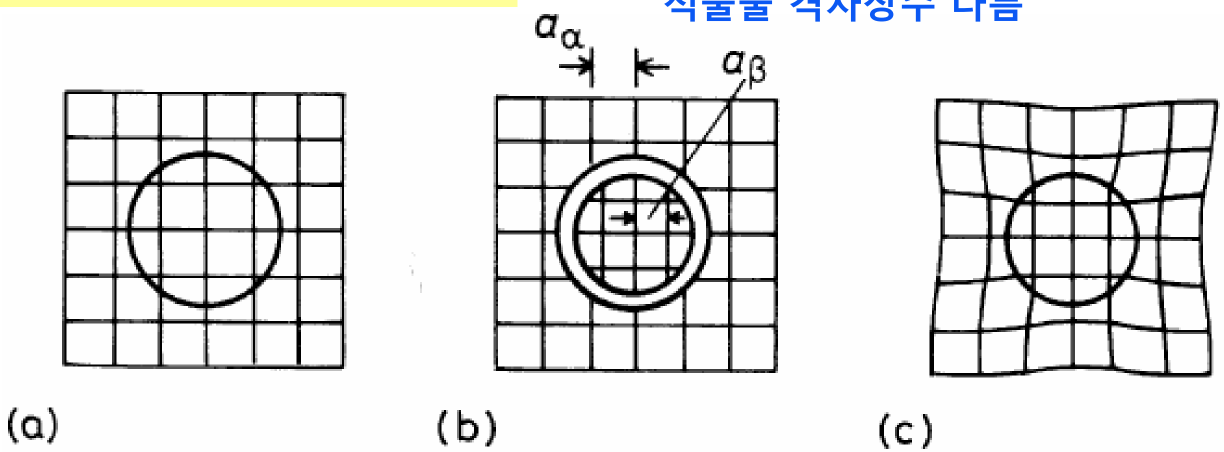


Fig. 3.47 The origin of coherency strains. The number of lattice points in the hole is conserved.

*Unconstrained Misfit*

$$\delta = \frac{a_\beta - a_\alpha}{a_\alpha}$$

⇨

*Constrained Misfit*

$$\varepsilon = \frac{a'_\beta - a_\alpha}{a_\alpha}$$

변형장에 의해 변화

$$\varepsilon = \frac{2}{3}\delta, \quad E_\beta = E_\alpha, \nu = 1/3$$

Poisson's ratio

실제, 기지와 다른탄성계수 $0.5\delta \le \varepsilon \le \delta, E_\beta \ne E_\alpha$

**if thin disc,**

석출물이 얇은 원판인 경우

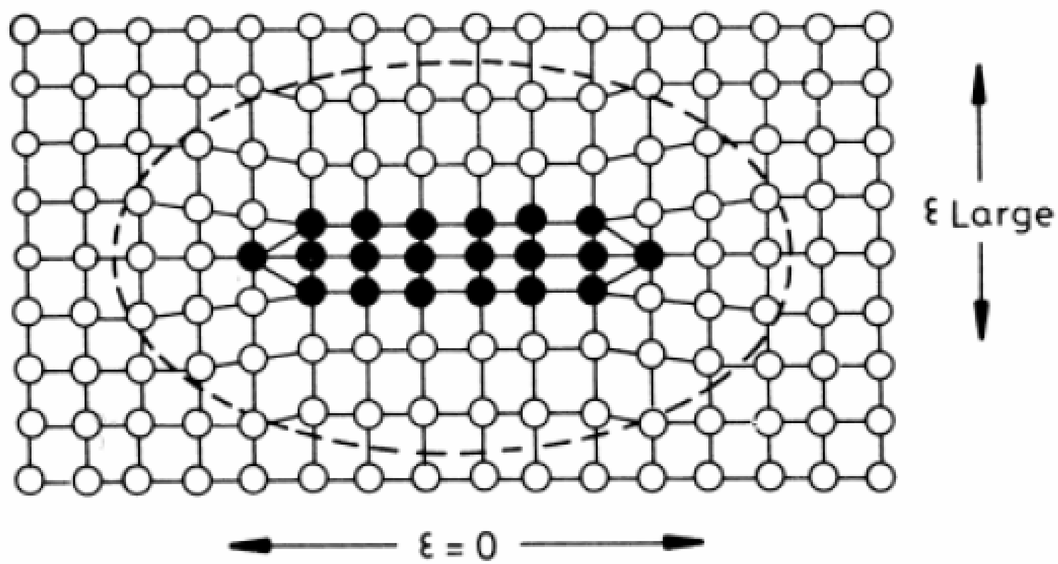


Fig. 3.48 For a coherent thin disc there is little misfit parallel to the plane of the disc. Maximum misfit is perpendicular to the disc.

총 탄성 에너지는 석출물의 모양과 기지와 석출물의 탄성 특성에 따라 변화

**Elastically Isotropic Materials** $\Delta G_S = 4\mu\delta^2 \cdot V$ (If ν=1/3)

석출물 모양에 무관

**Elastically Anisotropic Materials**

| | | | | |
|---|---|---|---|---|
| *Atom radius* ($\mathring{A}$) | $Al : 1.43$ | $Ag : 1.44$ | $Zn : 1.38$ | $Cu : 1.28$ |
| *Zone Misfit* ($\delta$) | – | $+ 0.7\%$ | $- 3.5\%$ | $- 10.5\%$ |
| *Zone Shape* | – | *sphere* | *sphere* | *disc* |

**Interfacial E effect dominant** $\delta < 5\%$ **strain E effect dominant**

탄성 변형 에너지 모양에 따라 변화

## B. Incoherent Inclusions

두 격자 계면이 연속성 상실/ 격자 불일치도 무의미해짐

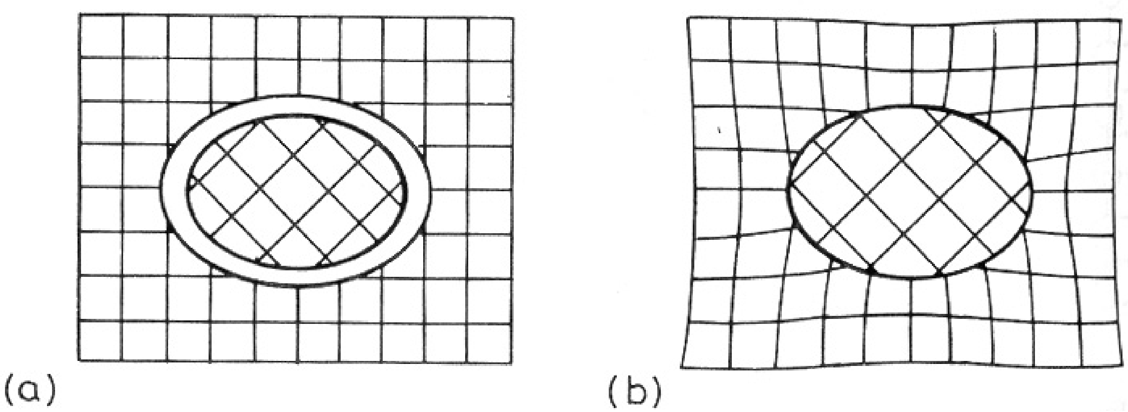


$$Volume\ Misfit \quad \Delta = \frac{\Delta V}{V}$$

Ex) 정합 구형 개재물 Δ=3δ

**For Elliptical Inclusions**

$$\frac{x^2}{a^2} + \frac{y^2}{a^2} + \frac{z^2}{c^2} = 1$$

Nabarro Eq.

**For a homogeneous incompressible inclusion in an isotropic matrix**

등방성 기지내
균일 비압축성 개재물의 탄성변형 E

$$\Delta G_S = \frac{2}{3}\mu\Delta^2 \cdot V \cdot f(c/a)$$

μ: the shear modulus of the matrix

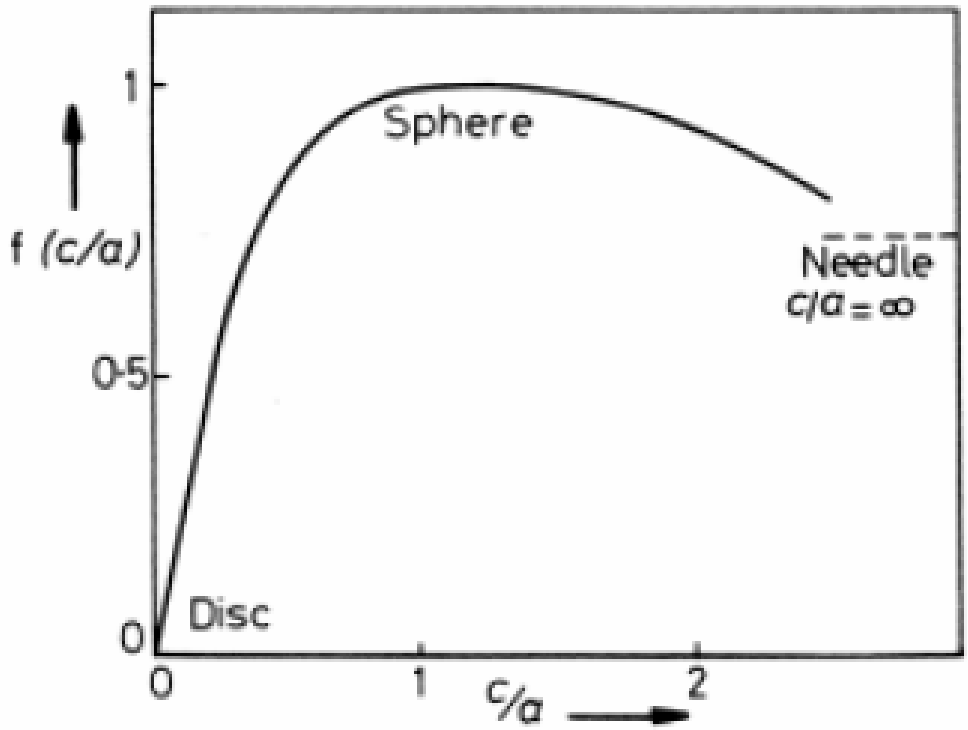


Fig. 3.50 The variation of misfit strain energy with ellipsoid shape, $f(c/a)$. (After F.R.N. Nabarro, *Proceedings of the Royal Society A*, **175** (1940) 519.)

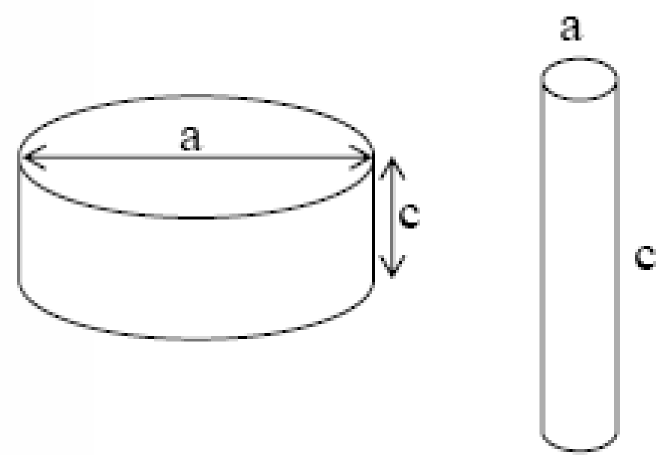


$$\Delta G_s = \frac{2}{3}\mu\Delta^2 \cdot V \cdot f(c/a) \qquad \Delta = \frac{V_\beta - V_\alpha}{V_\alpha} \approx 3\delta \text{ for sphere}$$

$$\neq 3\delta \text{ for disc or needle}$$

**부정합 개재물의 평형 모양: 계면 에너지와 변형 에너지의 상반 효과가 서로 균형을 이루는 c/a 값을 가지는 평평한 타원체**

## C. Plate-like precipitates

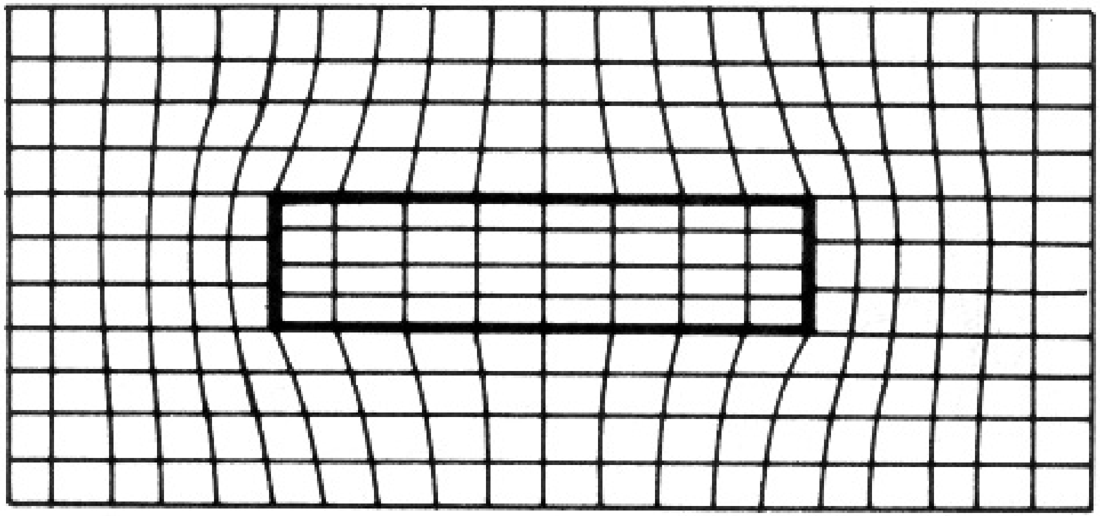

두께 증가시 넓은 면 가로질러 존재하는 구속된 불일치 증가

→ 기지 변형과 판 모서리에서의 전단응력 증가

→ 넓은 면 반정합 상태가 되는 것이 에너지적으로 바람직함

→ 불일치 변형에너지가 거의 없는 부정합 개재물 처럼 행동

Ex) Al-Cu 합금의 θ’ 상

# Coherency Loss

$$\Delta G(coherent) = 4\mu\delta^2 \cdot \frac{4}{3}\pi r^3 + 4\pi r^2 \cdot \gamma_{ch} \Leftrightarrow \Delta G(non-coherent) = 4\pi r^2 \cdot (\gamma_{ch} + \gamma_{st})$$

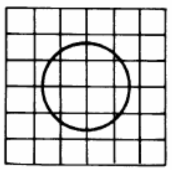

Coherency strain energy
Eq. 3.39

Chemical interfacial E

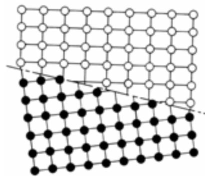

Chemical and structural interfacial E

$$\frac{4}{3}\pi r^3 (4\pi\mu\delta^2) + 4\pi r^2 (\gamma_{ch}) = 4\pi r^2 (\gamma_{st} + \gamma_{ch})$$

coherent $\qquad$ $\Delta G_s$-relaxed

$$\therefore r_{crit} = \frac{3 \cdot \gamma_{st}}{4\mu\delta^2}$$

$$\approx \frac{1}{\delta}$$

**($\delta = (d_\beta - d_\alpha)/ d_\alpha$ : misfit)**

$$for\ small\ \delta, \quad \gamma_{st} \propto \delta$$

**(semicoherent interface)**

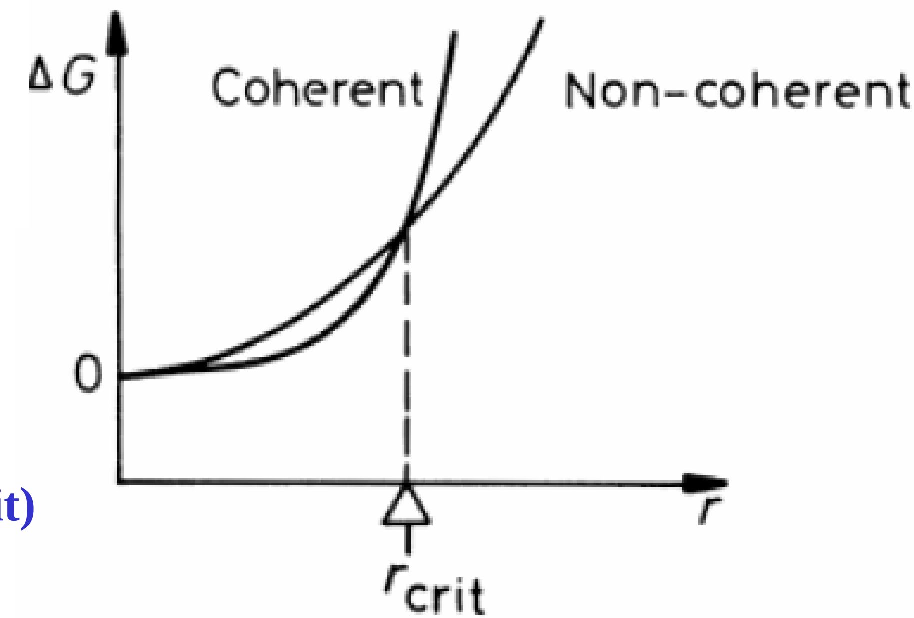


Fig. 3.52 The total energy of matrix + precipitate v. precipitate radius for spherical coherent and non-coherent (semicoherent of inchherent) precipitates.

**If a coherent precipitate grows, during ageing for example,**
**It should lose coherency when it exceeds $r_{crit}$.**

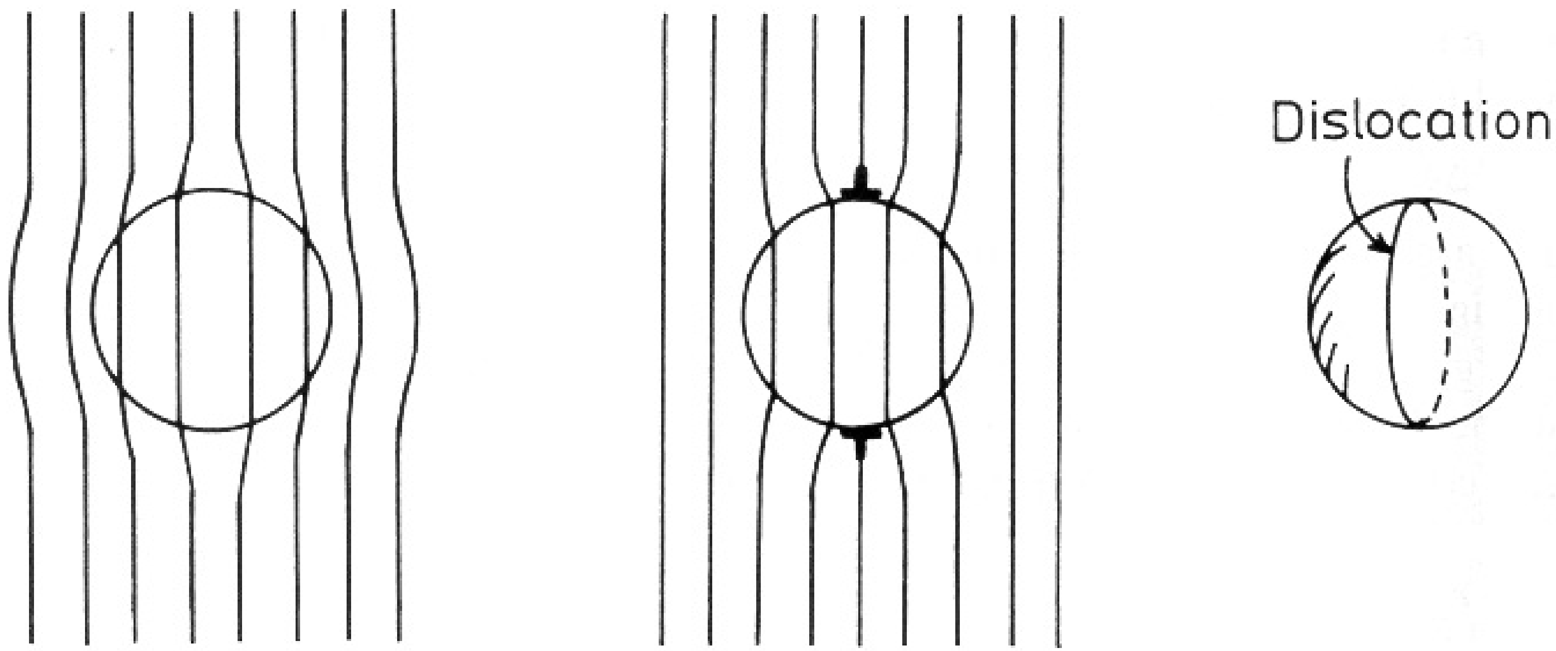


(a) **Coherent with strain E**

(b) **Coherency strain replace by dislocation loop.**

(c) **Precipitate with dislocation**

**Coherency loss for a spherical precipitate**

실제의 경우, 전위 루프 생성 어려움 → rcrit 보다 큰 크기의 정합 석출물 자주 관찰됨.

# Mechanisms for coherency loss

rcrit 보다 커지고, 계면에 이론강도를 초과할 정도의 응력이 계면에 생겨야 함

**spherical precipitate**

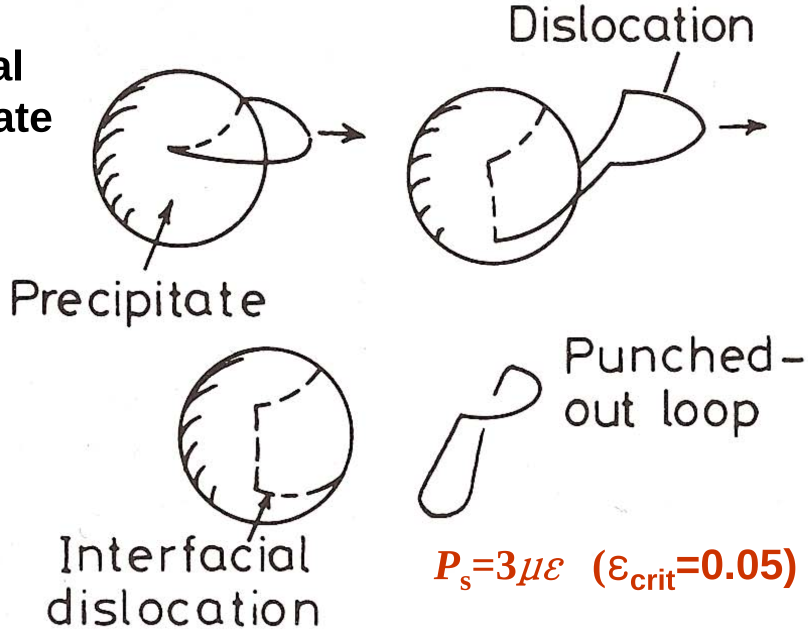


$P_s = 3\mu\varepsilon$ ($\varepsilon_{crit}$=0.05)

(a) 계면에서 전위를 생성

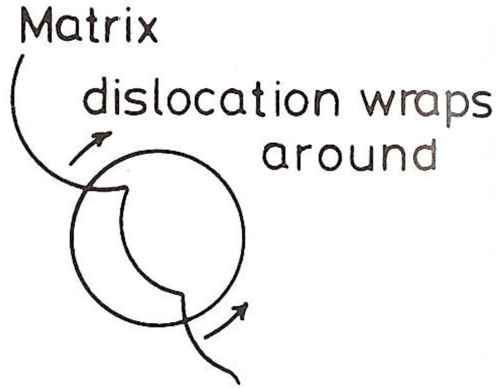


기계적 변형 커져서 전위밀도가 많은 경우

(b) 기지내 전위가 제2상의 계면으로 이동

**plate precipitate**

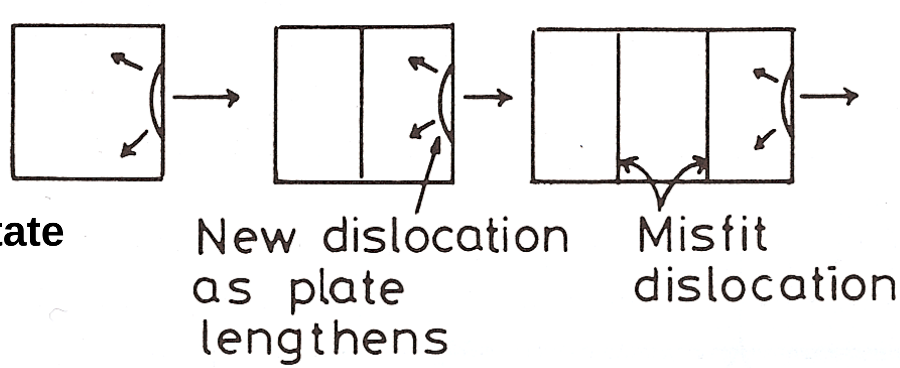


(c) 판상 제2상의 코너에서 전위가 생성되며
판이 넓어짐에 따라 전위 생성이 반복됨.

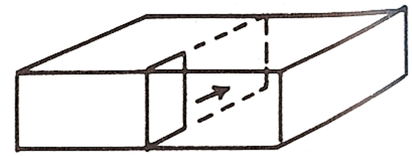

**Prismatic dislocation loop**

(d) 공공의 응축에 의해 제2상의 내부
전위루프가 커짐